

## Kinetic and Thermodynamic Studies on Adsorption of $Pb^{2+}$ and $Cr^{3+}$ from Petroleum Refinery Wastewater using Linde Type a Zeolite Nanoparticle.

Nwokem, Calvin Onyedika\*, Kantoma, Dogara , Zakka Israila Yashim and Zaharaddeen Nasiru Garba

*Received: 12 September 2023/Accepted: 17 January 2024/Published: 26 January 2024*

**Abstract:** In this research work, Linde type Zeolite (LTA-Zeolite) nanoparticles (ZANPs) were synthesized using kaolin obtained from Darazo Bauchi State, the X-ray fluorescence (XRF) result shows  $SiO_2$ ,  $Al_2O_3$  percentage of 60.247 and 38.316 respectively and  $SiO_2/Al_2O_3$  ratio of 1.57 which is suitable for the synthesis of Zeolite-A. The produced nano adsorbent was characterized using X-ray fluorescence (XRF), X-ray powder diffraction (XRD), scanning electron microscopy (SEM), Fourier transform infrared spectroscopy (FT-IR), Ultraviolet-visible spectroscopy (UV-visible spectroscopy) and  $N_2$ -Brunauer-Emmett-Teller (BET) surface analysis. The SEM micrographs revealed well-dispersed Zeolite-A nanoparticles (ZANPs) and the  $N_2$ -BET showed a high surface area of  $106.250\text{m}^2/\text{g}$ , pore diameter of 2.1132 (nm) and a pore volume of 0.052 (cc/g) for ZANPs. The array of removal of Heavy metal pollutants Pb, 96.0% Cr, 90%, ZANPs removing a higher percentage of Lead pollutants. Isothermal models indicated that the Freundlich model ( $R^2$ ) of 0.999 was most suitable for describing the adsorption process, which conformed to pseudo-second-order kinetics ( $R^2$ ) of 0.999Cr.

**Keywords:** Remediation, heavy metal, nanoparticles, zeolites; petroleum industrial wastewater

**Nwokem, Calvin Onyedika \***

Department of Pure and Applied Chemistry, Kaduna State University, Nigeria

**Email:** [onyenwokem@gmail.com](mailto:onyenwokem@gmail.com)

**Orcid id:** 0009 0001 0220 0714

**Kantoma, Dogara**

Department of Applied Chemistry, Kaduna Polytechnic, Kaduna, Nigeria

**Email:** [kantomadogara@gmail.com](mailto:kantomadogara@gmail.com)

**Orcid id:** 0000 0001 2345 6789

**Zakka Israila Yashim**

Department of Chemistry, Ahmadu Bello University Zaria, Nigeria, Kaduna State, Nigeria

**Email:** [zakkayashim@gmail.com](mailto:zakkayashim@gmail.com)

**Orcid id:** 0000 0002 9103 2301

**Zaharaddeen Nasiru Garba**

Department of Chemistry, Ahmadu Bello University, Zaria, Nigeria

**Email:** [dinigetso2000@gmail.com](mailto:dinigetso2000@gmail.com)

**Orcid id:** 0000 0001 7265 9048

### 1.0 Introduction

Based on the World Health Organization findings, the volume of contaminated water in the global society is several times more than the volume of potable water (Eddy *et al.*, 2023a-b; Jimoh and Umar, 2015). Several point and non-point pollution sources have been investigated and such results have always led to the conclusion that industrial activities are the major sources of contaminants in most of our water sources (Adefemi and Awokunmi, 2007). The consequence could range from mild symptoms to chronic and finally death (Deziel & Villanueva, 2024). Among the notable industries, whose contamination problems have been significantly published is the petroleum industry. (Ugya *et al.*, 2017). Several hydrocarbon, heavy metal, other organics and physicochemical parameters of

water contaminated with wastes from the petroleum sectors have never been favourable to man and the environment (Dey and Islam, 2015). In the water sector, such observations have been widely targeted by the development of different water treatment measures including adsorption, photodegradation, electrophoresis, electro dialysis, ozonation, oxidation, etc (Tijjani *et al.*, 2014; Garg *et al.*, 2022). Adsorption is generally accepted as a sound measure because of its flexibility regarding cheap raw materials options, cost-effectiveness, biodegradability and environmentally friendliness. (Ibrahim and Abdullahi, 2017) However, the right choice of adsorbent can be a major challenge towards the success of achieving optimum or complete removal of contaminants (Baral *et al.*, 2021). Widely acceptable properties of good adsorbent borders on surface properties such as large surface area, high porosity, large surface area to volume ratio high thermal stability and resistance to chemical attack as well as mechanical stability (Ibrahim and Abdullahi, 2017). Over some decades, investigative reports suggest that most materials can meet some of the listed conditions but nanoparticles are unique when considering the listed conditions (Makarov *et al.*, 2014; Odoemelam *et al.*, 2023). Recently, nanomaterials have been considered good materials for wastewater treatments (Shannon *et al.*, 2008). However, it is reported that, when the size of the metal decreases to the nanometer range, the increased surface energy leads to their poor stability (Lee *et al.*, 2015; Baqer *et al.*, 2017). Since heavy metals are one of the most endangering contaminants in aquatic systems, their presence in petroleum wastewater is significantly unacceptable. Therefore, there is a need to offer an effective remediation approach. Therefore, this study is aimed at synthesizing zeolite A type from kaoline obtained from some locations in Nigeria.

## 2.0 Materials and Methods

The wastewater was collected from the Kaduna Refinery and Petrochemical Company (KRPC) in Kaduna, Kaduna state. The kaolin used in this research work was collected from Fate Darazo Local Government Area in Bauchi state, Nigeria. Both distilled and deionized water were used throughout the laboratory studies as well as sample treatment and analysis.

### 2.1 Pre-treatment of the raw Kaolin

The refining or treatment process started by crushing 700 g of the raw Fate-Darazo kaolin using a porcelain mortar and pestle. It was soaked in 15 litres of water for 24 hours to form a slurry, and dissolve impurities and other unwanted materials present (slurry) at the top surface water was decanted and the slurry was sieved with a sieve of mesh size 350 $\mu$ m and then air dried. The dried cake was pulverized and sieved to allow only particles with sizes  $\leq$  100 $\mu$ m to pass through and characterized using XRF, XRD, FTIR and SEM.

### 2.2 Metakaolinization process

The meta-kaolinization process was carried out by subjecting the sample to elevated temperatures ranging from 600 to 900 °C for 2 hours using a muffle furnace (Mgbemere *et al.*, 2018). It was characterized using XRF.

### 2.3 Synthesis of LTA-zeolite from kaolin

Synthesis of zeolite was carried out using the metakaolin sample calcined at 700 °C and 900°C while NaOH Pellets as the source of Na<sub>2</sub>O. Using 6 g of NaOH dissolved in 100 cm<sup>3</sup> of deionized water and stirred briefly for 10 minutes. 5 g of metakaolin was then added gently to obtain the aluminosilicate gel. The gel was stirred continuously at room temperature allowed to age for 24 hours and transferred into a 100 ml stainless autoclave.

A hydrothermal treatment was performed in an oven (Model No:0607034; 2006-2007) maintained at 120°C for 6 hours. At the end of the hydrothermal reaction, the mixture was



filtered and washed with deionized water until a pH of about 7 was obtained and dried in an oven at 100°C for 4 hours and calcined in a furnace (Model SXL Muffle furnace). The ZeoliteA obtained was characterized using FTIR, XRD, EDS and SEM.

**2.4 Batch Adsorption Experiment**

A batch adsorption study was employed. Equilibrium isotherms were obtained by studying the adsorption process of Lynde type A Zeolite(LTA-zeolite) at different contact times, temperatures and adsorbent dosages. The effect of contact time was studied to establish the adsorption equilibrium. The effects of temperature were studied to evaluate the adsorption kinetics parameters and the effects of adsorbent dosage were also to investigate adsorption isotherms.

Adsorption equilibrium and percentage removal were calculated using equations 1 and 2 respectively (Eddy *et al.*, 2024a-b)

$$q_e = \frac{C_1 - C_2}{1} \times \frac{V}{m} \quad (1)$$

$$q_e = \frac{C_1 - C_t}{1} \times \frac{V}{m} \quad (1)$$

$$\% \text{ Removal } (R) = \frac{C_1 - C_2}{C_1} \times \frac{100}{1} \quad (3)$$

$q_e$  is the amount of adsorbate adsorbed at equilibrium (mg/g),  $C_1$  is the amount of adsorbate

adsorbed at time  $t$ .  $C_1$ ; the initial adsorbate concentration in (mg/L),  $C_2$ ; the concentration of adsorbate at equilibrium (mg/L),  $m$  is the mass of adsorbent (g) and  $V$ ; the volume of the solution (mL) (Ibrahim and Abdullahi, 2017).

**2.5 Regeneration studies**

The desorption of Pb, and Cr, loaded into ZANPs and regeneration of the ZANPs adsorbent were performed four times using 0.002 M HNO<sub>3</sub> to study the reusability of the prepared nanoadsorbent. Then, the ZANPs adsorbent was separated using filter paper washed four times with deionised water and dried at 60°C overnight for reuse. This process was repeated three times (Abdullah *et al.*, 2017).

**3.0 Results and Discussion**

**3.1 Characterization of Kaolin**

Samples of kaolin were analysed for SiO<sub>2</sub>/Al<sub>2</sub>O<sub>3</sub> ratio using X-ray fluorescence (XRF) and the results obtained are shown in Table 1 below. The samples were taken from Darazo, Kankara and Bida. The presented results indicate that the Al<sub>2</sub>O<sub>3</sub> and SiO<sub>2</sub> constituted up to 95% of the analysed kaolin samples.

**Table 1: XRF Analysis of Darazo (Fate), Kankara and Bida raw kaolin (weight%) ).**

Oxides	Darazo	Kankara	Bida
SiO <sub>2</sub>	60.247	55.090	56.210
Al <sub>2</sub> O <sub>3</sub>	38.316	38.935	36.549
V <sub>2</sub> O <sub>5</sub>	0.001	0.351	0.137
Cr <sub>2</sub> O <sub>3</sub>	0.007	0.011	0.045
MnO	0.049	1.084	0.048
Fe <sub>2</sub> O <sub>3</sub>	0.379	1.224	1.763
Co <sub>3</sub> O <sub>4</sub>	0.005	0.003	0.007
NiO	0.005	0.309	0.011
CuO	0.035	0.033	0.032
Nb <sub>2</sub> O <sub>3</sub>	0.014	0.012	0.013
MoO <sub>3</sub>	0.003	0.003	0.001
WO <sub>3</sub>	0.003	0.006	0.000
P <sub>2</sub> O <sub>5</sub>	0.000	0.000	0.101
SO <sub>3</sub>	0.073	0.000	0.062



CaO	0.078	1.390	0.138
MgO	0.000	0.000	0.000
K <sub>2</sub> O	0.000	0.559	0.516
BaO	0.076	0.136	0.165
Ta <sub>2</sub> O <sub>5</sub>	0.050	0.024	0.014
TiO <sub>2</sub>	0.056	0.190	3.271
ZnO	0.005	0.007	0.004
Ag <sub>2</sub> O	0.042	0.010	0.019
Cl	0.043	0.604	0.578
ZrO <sub>2</sub>	0.114	0.017	0.316
Total	100%	99.998%	100%
SiO <sub>2</sub> /Al <sub>2</sub> O <sub>3</sub>	1.57	1.43	1.53

For Darazo (Fate), Kankara and Bida kaolin, the SiO<sub>2</sub> and Al<sub>2</sub>O<sub>3</sub> amounts are 60.247 and 38.316% respectively, Kankara 55.090 and 38.935% respectively while that of Bida

sample the values are 56.210 and 36.549% respectively.

The elemental composition of the untreated, treated and metakaolin produced from Fate-Darazo kaolin is presented in Table 2.

**Table 2: Elemental composition of Untreated, Treated and metakaolin**

Oxides	Untreated (%)	Kaolin	Treated(%)	Metakaolin(%)
SiO <sub>2</sub>	54.501		51.398	51.035
Al <sub>2</sub> O <sub>3</sub>	41.463		40.003	40.365
V <sub>2</sub> O <sub>5</sub>	0.034		0.186	0.206
Cr <sub>2</sub> O <sub>3</sub>	0.006		0.000	0.025
MnO	0.064		0.041	0.016
Fe <sub>2</sub> O <sub>3</sub>	1.603		0.934	1.179
Co <sub>3</sub> O <sub>4</sub>	0.010		0.003	0.010
NiO	0.011		0.005	0.003
CuO	0.043		0.040	0.067
Nb <sub>2</sub> O <sub>3</sub>	0.011		0.147	0.143
MoO <sub>3</sub>	0.003		0.000	0.000
WO <sub>3</sub>	0.000		0.000	0.015
P <sub>2</sub> O <sub>5</sub>	0.000		0.000	0.015
SO <sub>3</sub>	0.000		0.205	0.000
CaO	0.525		0.743	2.166
MgO	0.000		0.000	0.000
K <sub>2</sub> O	0.714		0.035	0.167
BaO	0.088		0.268	0.319
Ta <sub>2</sub> O <sub>5</sub>	0.028		0.039	0.025
TiO <sub>2</sub>	0.211		4.059	4.001
ZnO	0.008		0.003	0.034
Ag <sub>2</sub> O	0.011		0.008	0.018
Cl	0.024		0.758	1.517



ZrO <sub>2</sub>	0.041	0.758	0.795
SnO <sub>2</sub>	0.000	0.000	0.000
<b>Total</b>	99.858%	100%	100%
SiO <sub>2</sub> /Al <sub>2</sub> O <sub>3</sub>	1.31	1.28	1.26

The results revealed the presence of SiO<sub>2</sub> and Al<sub>2</sub>O<sub>3</sub> as the main constituents. It further shows the reduction in SiO<sub>2</sub> content of the untreated, treated and metakaolin, a decrease in treated and an increase in Al<sub>2</sub>O<sub>3</sub> of metakaolin respectively. The percentage of SiO<sub>2</sub> decreased from 54.50 to 51.04% and Al<sub>2</sub>O<sub>3</sub> increased from 37.44 to 40.37% for treated and metakaolin, respectively.

**3.2 Characterization of the adsorbent.**

addition to XRD in the treated, untreated and metakaolin, the adsorbent was also characterised by XRD, SEM, EDX and FTIR, BET, UV-visible. The XRD pattern of the metakaolin, treated and untreated kaolin are shown in Fig.1,.2 and 3 respectively. . The result shows that the main peaks at  $2\theta = 12.24^\circ$  and  $24.76^\circ$  which were the main peaks in identifying kaolinite in refined kaolin were no longer observed in the metakaolin diffraction pattern.

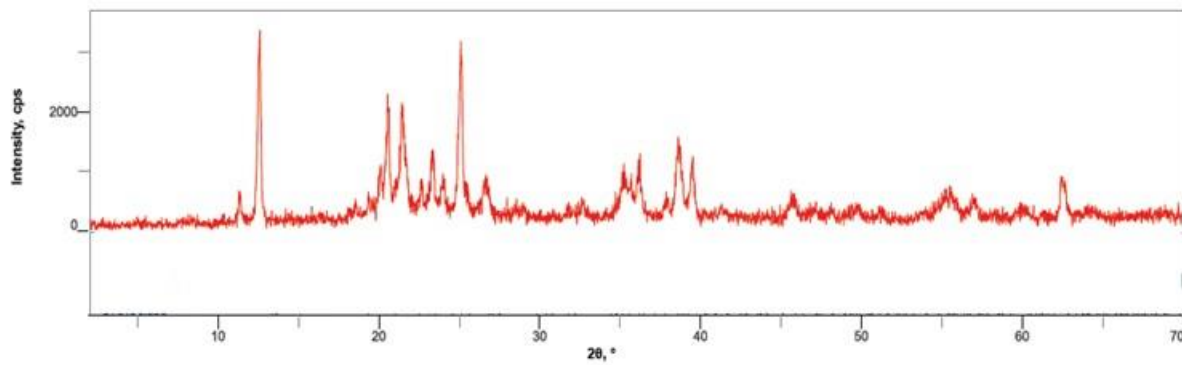


**Fig. 1: XRD pattern of Metakaolin**

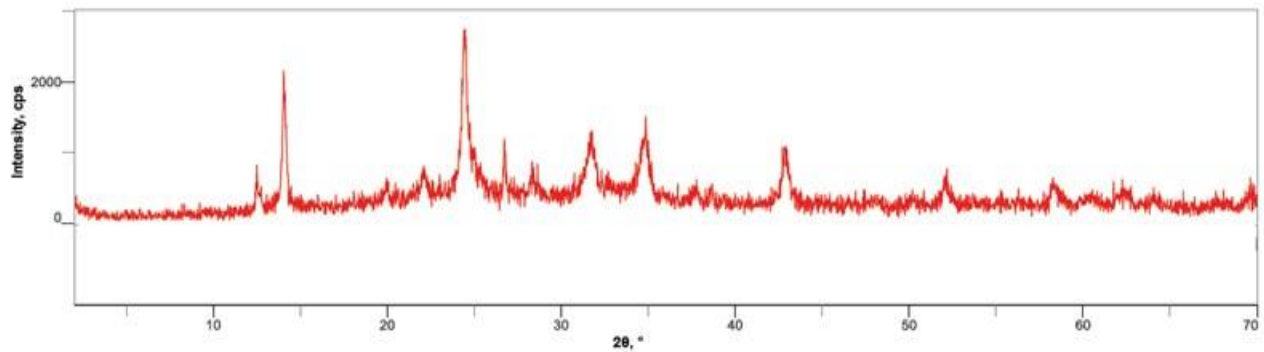


**Fig.2: XRD pattern of treated kaolin**



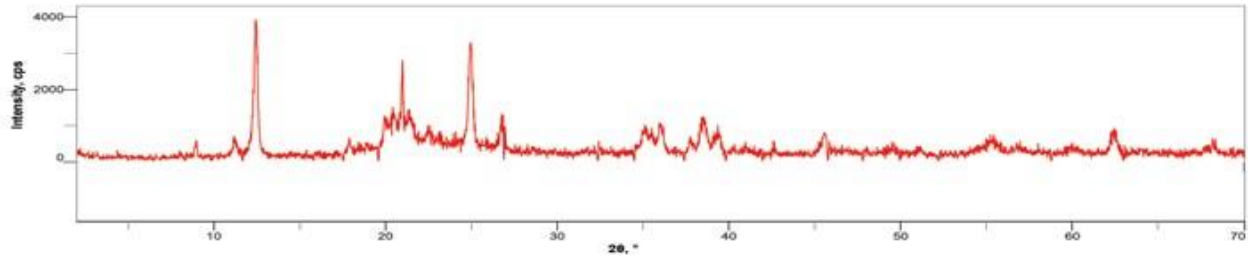


**Fig. 3: XRD pattern of untreated kaolin**

The observation of samples by SEM (image) Fig. 4 reveals little porosity on the surface before adsorption, this could promote the adherence of the metal in molecules. Fig. 5 reveals tiny pore spaces on the surface after adsorption, this is caused by filling in gaps

in the zeolite A by the adsorbate deposited molecules. Also, Data obtained from EDS of the zeolite are shown in Table 3. The results indicate a high concentration of carbon (85.34%) and oxygen (11.11%)

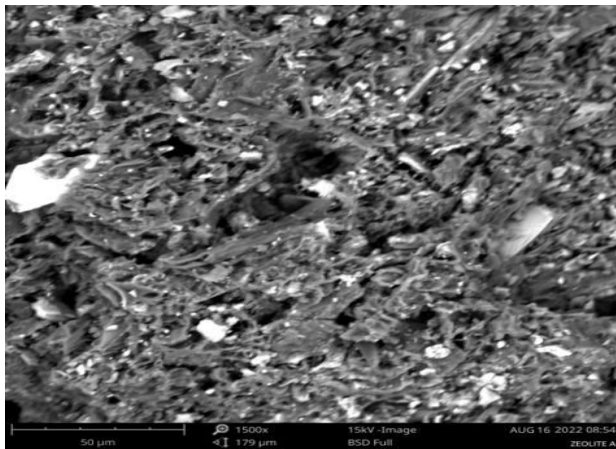


**Fig. 4: SEM micrograph of Zeolite A nanoparticle before adsorption**

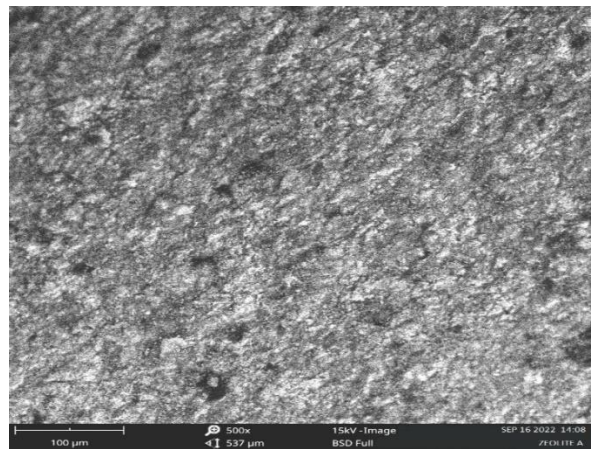


**Fig. 5: SEM micrograph of Zeolite A after adsorption**

**Table 3: Energy Disperse Spectroscopy (EDS) of zeolite A.**

Element Number	Element Symbol	Element Name	Atomic Conc.	Weight Conc.
6	C	Carbon	85.34	78.80
8	O	Oxygen	11.11	13.66
14	Si	Silicon	0.58	1.25
7	N	Nitrogen	1.00	1.08
26	Fe	Iron	0.23	0.98
19	K	Potassium	0.32	0.97
13	Al	Aluminium	0.32	0.67
20	Ca	Calcium	0.20	0.61



12	Mg	Magnesium	0.26	0.49
15	P	Phosphorus	0.20	0.47
16	S	Sulfur	0.16	0.40
17	Cl	Chlorine	0.12	0.32
11	Na	Sodium	0.17	0.29

EDX was employed to determine the elemental characterization of zeolite nanoparticles samples, before adsorption. From the result (Table 3), carbon showed the highest elemental percentage of 85.34 followed by oxygen with 11.11% . The observed results are consistent with the works published by (Sherifat *et al.*, 2019).

Fig. 6, the FT-IR of the zeolite A sample is

shown. Observed peaks and the frequencies, they occurred as well as the assignment are presented in Table 4. Notably, the FTIR spectrum displayed a characteristics peak that is known to zeolite nanoparticles at  $3339.7\text{cm}^{-1}$  which is the O-H bond representing the hydroxyl group of water molecules present in zeolitic pores spaces. It also depicts aldehydes and phenols functional groups.

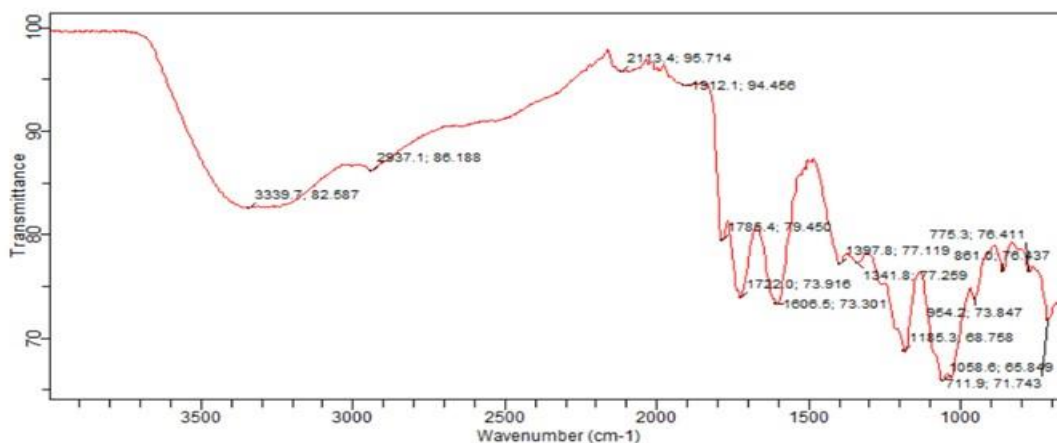
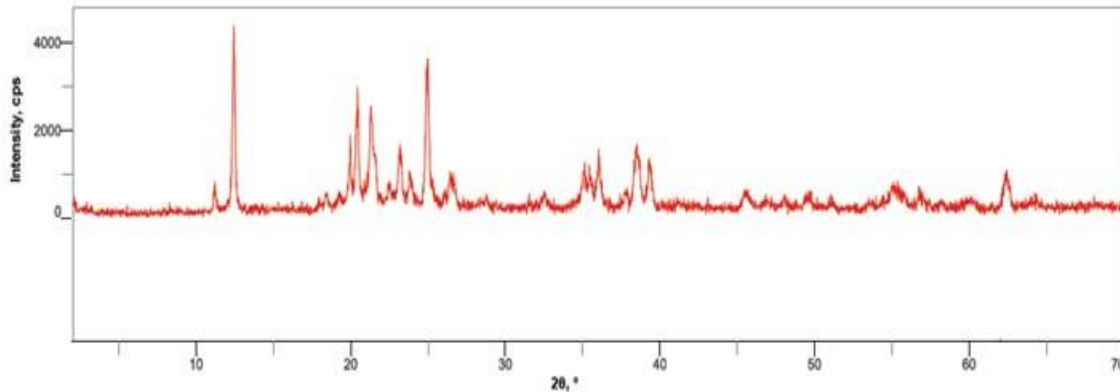


Fig.6: FT-IR pattern of ZeoliteA.

Table 4 :Results of FT-IR of Synthesized Zeolite-A

S/NO.	Peaks ( $\text{cm}^{-1}$ )	Bond	Functional groups
1.	3340	O – H	Hydroxyl group
2.	2937	N – H stretch	Amines
3.	2143	O – H stretch-free hydroxyl OH.	Aldehydes, phenols
4.	1912	– C $\equiv$ C – stretch	Hydroxyl group, lipids
5.	1785	– C – O – stretch	Alkyne
6.	1722	– N – O asymmetric stretch	Nitro cards
7.	1398	– C – H bond	Alkane





**Fig.7: XRD pattern of ZeoliteA**

The result of the phase composition investigated by x-ray diffractometer is presented in Fig.7 for zeoliteA nanoparticle sample, the XRD pattern obtained from the quantitative analysis report showed a visible sharp peak around 2 theta as this proves the phase nature of the solid to be a crystalline solid.

**Table 5: BET analysis of synthesized zeoliteA adsorbent**

Adsorbent	surface area(m <sup>2</sup> /g)	Pore Diameter (nm)	Pore Volume (cc/g)
ZANPs	106.250	2.132	0.052

ZeoliteA exhibited isotherm adsorption behaviour due to the presence of zeolitic micropores, (Abdallah *et al.*,2017), as well as mesopores formed by the aggregation of crystals which are in agreement with the SEM image (Fig. 4. and 5).

The UV spectra obtained for the biosynthesis of zeolites as shown in. Fig. 8. A colour change from light yellow to white was observed after the reaction time, which is an indication of the formation of zeolite A

The characterization of the adsorbent with the UV –Spectrophotometer was carried out in the range of 190-240nm. The strong surface

Plasmon resonance (SPR) band position at 210nm was observed for the ZANPs, (fig. 8). The position of SPR is sensitive to particle shape, size and interaction with the medium

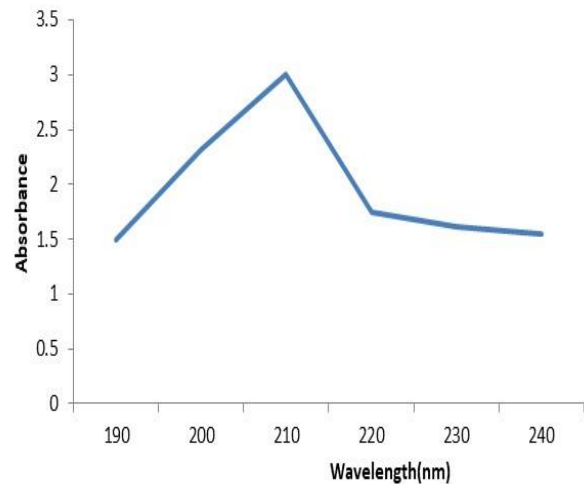


**Fig. 8: UV-Vissible Spectroscopy of zeolite A nanoparticles.**

and the particle (Ibrahim and Abdullahi 2017).The broad spectra indicate that there is a mixture of particles (Sosa *et al.*,2003).

**3.3 Adsorption Study**

The result in Fig. 9: below shows the extent of Pb, Cr removal by ZANPs, it was found to increase with increasing the contact time each a maximum value after 10 min. With Pb having the highest % Removal of 60%.





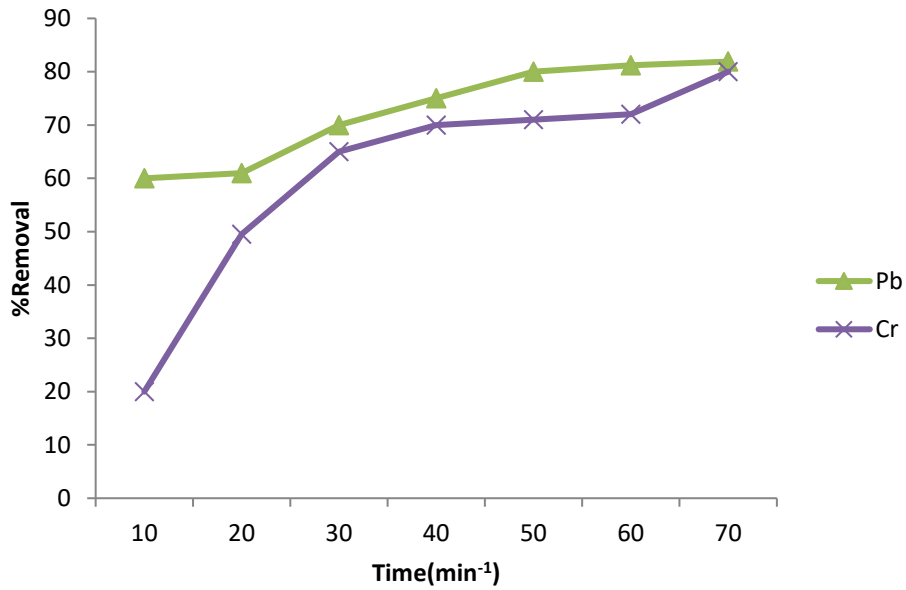


**Fig. 9: Variation of percentage removal of Pb<sup>2+</sup> and Cr<sup>3+</sup> by ZANPs with time ( at a temperature =40°C, speed =300rpm,pH = 4 and adsorbent dosage of 1.0g/50ml)**

The amounts of Pb, Cr adsorbed by different amounts of ZANPs adsorbent are shown in Fig. 9. The increase in adsorbent dosage from 0.2

to 1.0 g increased the adsorptions percentage of Pb<sup>2+</sup>, Cr<sup>3+</sup> with Cr having the highest % Removal of 90%.

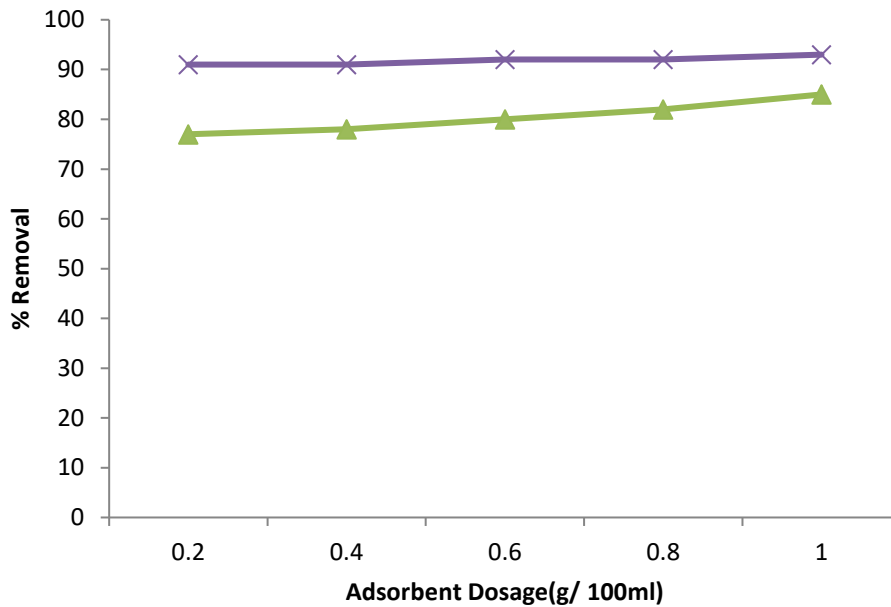


**Fig.10: Result on effect of Adsorbent Dosage on removal of Chemical parameters onto ZANPs, (temperature=40°C, speed=300rpm, pH =4 and time 30min.)**



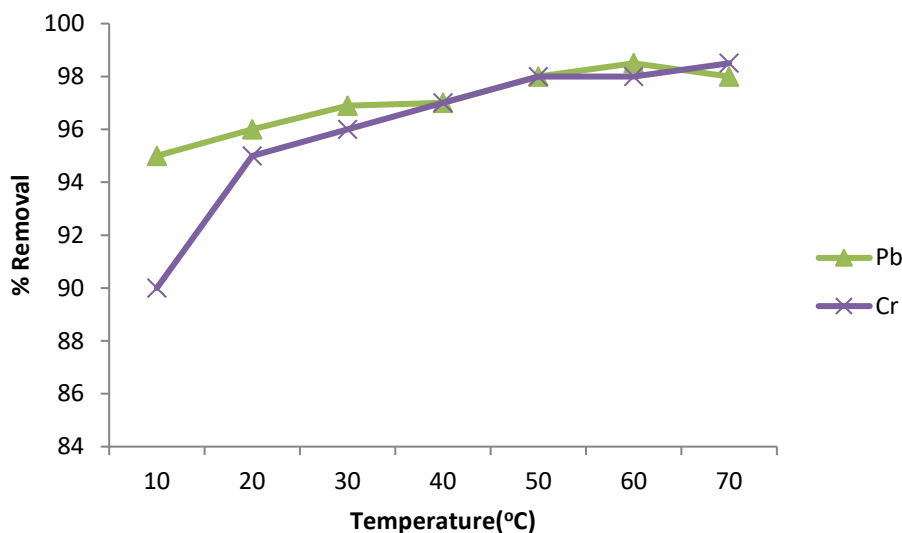


**Fig. 11: Result on the effect of temperature on removal of Chemical parameters onto ZANPs, (Adsorbent Dosage= 1.0 g/ml, speed=300rpm, pH =4 and time 30min.)**

The results obtained are presented in Fig. 8. The Fig. 8 result revealed that the adsorption rate of the chemical parameters onto ZANPs increased with an increase in temperature in all cases. This is attributed to the immobility of the chemical parameters molecules as the temperature increased, which subsequently; resulted in the formation of a strong binding force between the contaminants and the zeolites A (Acemioglu, 2010; Al-Anber, 2011; Yusuf-Alaya, 2014; Bankole *et al.*, 2017). The result depicts that Pb has the highest percentage removal at 94%. This is in agreement with the result reported by (Sherifat *et al.*,2019)

**3.4 Kinetics and adsorption isotherms**

Kinetics models such as pseudo-first-order and pseudo-second-order kinetics were applied in this research for testing the experimental data which conformed to pseudo-second order as shown in Table 6. Two isotherm models were tested and the parameters are shown in Table 5. From the results (Table 5), R<sup>2</sup> value of the Freundlich isotherm model was higher than the Langmuir model, this explains that the experimental equilibrium data fitted better by the Freundlich equation.

**Table 5: Adsorption parameters for the removal of Pb<sup>2+</sup> and Cr<sup>3+</sup> by adsorption onto ZANPs at pH = 4**

Adsorption Isotherms	Pb	Cr
Langmuir		
q <sub>e(exp)</sub> (mg/L)	0.901	0.751
q <sub>m</sub> (mg/g)	0.847	0.653
K <sub>L</sub> (L/g)	7.687	5.032
R <sub>L</sub>	0.014	0.022
R <sup>2</sup>	0.983	0.960



Freudlich		
1/n	0.121	0.070
$K_f(L/g)$	0.284	0.456
$R^2$	0.999	0.959
Harkin-Jura		
B	0.072	0.086
A	0.695	0.678
$R^2$	0.967	0.977

**Tale 6: Kinetics kinetic parameters for the removal of Pb<sup>2+</sup> and Cr<sup>3+</sup> by adsorption onto ZANPs at pH = 4**

Pseudo-first order				Pseudo-second order			
Contaminan	$k_1(\text{min}^{-1})$	$q_e(\text{mg/g})$	$R^2$	$k_2(\text{min}^{-1})$	$q_{e(\text{cal})}(\text{mg/L})$	$q_{e(\text{exp})}(\text{mg/L})$	$R^2$
Pb	3.701	0.071	0.959	0.554	0.016	0.009	0.991
Cr	0.439	0.008	0.982	0.398	0.211	0.111	0.999

**Table 7: Intraparticle diffusion model for ZANPs and MDZA-NCs onto the conterminant**

Contaminant	$K_m(\text{mg/g min}^{1/2})$	C (mg/g)	$R^2$
ZANPs			
Pb	10.60	38.08	0.998
Cr	9.218	24.02	0.009

**Key:**  $k_1$ : Pseudo first-order rate constant,  $K_2$ : Pseudo -second-order rate constant,  $q_e$ : Equilibrium adsorption capacity,  $q_t$ : Adsorption capacity at time  $t$ ,  $t$ : Adsorption time,  $k_{diff}$ : Intraparticle diffusion rate constant,  $C$ : Intercept which is related to the thickness of the boundary layer

The thermodynamic parameters such as Gibb’s free energy,  $\Delta G^\circ$ ; the enthalpy  $\Delta H^\circ$  and the entropy  $\Delta S^\circ$  (Table 9 and 10) were also evaluated using the Transition state plots and the Gibb Helmholtz equation (Eddy *et al.*, 2024a-b). These parameters are vital for the determination of the feasibility of the adsorption process. The equilibrium constant of adsorption was evaluated using equation 4 (Liu, 2009; Bankole *et al.*, 2017). However, the the enthalpy and entropy changes were evaluated using equation 5 while the free energy change was calculated using equation 6.

$$k = \frac{q_e}{C_e} \tag{4}$$

$$\ln(k/T) = \frac{R}{Nh} + \frac{\Delta S^\circ}{R} - \frac{\Delta H^\circ}{RT} \tag{5}$$

$$\Delta G_{ads}^* = -RT \ln k_e = -RT \ln(k) \tag{6}$$

$k$  is the equilibrium constant;  $q_e$  and  $C_e$  are the equilibrium concentrations of the chemical parameters (mg/L) in solution and on the adsorbents, respectively. The plots of  $\ln K$  vs.  $1/T$  are shown in Fig. 12 and  $\Delta H^\circ$  and  $\Delta S^\circ$  were evaluated from the slopes and intercepts are shown in Table 9. It can be deduced from the results obtained that the adsorption process is endothermic since the obtained values of enthalpy are positive. The adsorption process also occurred with increasing degree of association since the negative values of entropy change indicate increase in orderliness. We also observed that the free energy change are negative which confirmed that the adsorption is



spontaneous. However, based on the magnitude of the free energy change, adsorption can be regarded as a physical or chemical mechanism. Values of free energy change negatively less than -40 kJ/mol are representative of physical adsorption and those negatively higher than -40 kJ/mol are indications of chemisorption data. Based on the results obtained in this study, it is significant to

state that the adsorption mechanism is chemisorption. The pattern of relationship obtained from the experimental data showing the variation of % removal with temperature also indicated that the adsorption increases with an increase in temperature, which is a confirmation for chemical adsorption

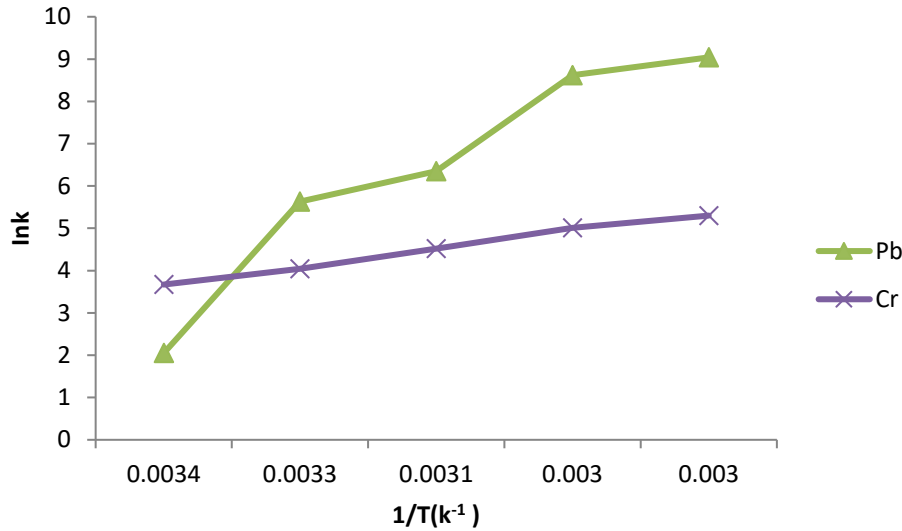


Fig. 12:A plot of lnk versus 1/T for ZANPs.

Table 8: k- values of sorption for chemical parameters onto ZANPs at various degrees of temperatures

Contaminant	20° C	30° C	40° C	50° C	60° C
Pb	1.89	5.20	6.01	7.16	8.40
Cr	35.36	50.65	65.10	100.01	120.14

Table 9: Adsorption thermodynamics of chemical parameters onto synthesized ZANPs

Contaminants	ΔH° (kJ/mol)	ΔS° (kJ/mol)
Pb <sup>2+</sup>	12.47	-10.31
Cr <sup>3+</sup>	2.49	-27.44

Table 10: ΔG° Free energies of the contaminant after adsorption by ZANPs at various temperatures

T (°C)	Pb <sup>2+</sup>	Cr <sup>3+</sup>
20	-218.77	-551.29
30	-296.80	-825.65
40	424.83	-1100.02
50	-527.92	-1374.37
60	-631.02	-1648.73



#### 4.0 Conclusion

This study successfully synthesized zeolite A nanoparticles (ZANPs) from kaolin sourced from Fate-Darazo, Nigeria, and investigated their potential for removing lead (Pb) and chromium (Cr) from petroleum wastewater. The characterization results confirmed the formation of zeolite A with a high surface area and the presence of functional groups suitable for adsorption. Batch adsorption experiments revealed that ZANPs effectively removed Pb and Cr, with Pb showing a higher removal efficiency (up to 94%) compared to Cr (up to 90%). The adsorption capacity increased with increasing contact time, adsorbent dosage, and temperature. Kinetic studies indicated that the adsorption process followed a pseudo-second-order model. The Freundlich isotherm model better described the equilibrium data, suggesting a multi-layered adsorption process. Thermodynamic parameters revealed a spontaneous and feasible adsorption process with an exothermic nature. Overall, this study demonstrates the promising potential of ZANPs synthesized from local kaolin for remediating heavy metal contamination in petroleum wastewater. We also recommend that further study in exploring the reusability and regeneration cycles of ZANPs for cost-effective application. Investigation of the effect of co-existing ions and real wastewater matrices on the adsorption performance as well as scaling up the synthesis process for pilot-scale and real-world applications are also recommended for future research.

#### 5.0 References

- Alswata, A. A., Ahmad., M. B., Al-Hada., M. N., Kamari., H. M., Bin Hussein, M. Z. & Azowa, N. (2017). Preparation of zeolite/zinc oxide nanocomposites for toxic metals removal from water. *Result in Physics*, 7, pp. 723-731.
- Adefemi, S. O. & Awokunmi, E.(2007).Assessment of the physico-chemical status of water samples from major dams in Ekiti State, Nigeria. *Pak. Nut.* 6,6, pp 657-659.
- Al-Anber, M. A. (2011). Thermodynamics approach in the adsorption of heavy metals. *In Thermodynamics -Interaction Studies - liquids and Gases*, ed Dr.Juan Carlos Moreno Piraján, 736–761, *InTech*.
- Bankole, M. T., Abdulkareem, A. S., Tijani, J. O., Ochigbo, S. S., Afolabi, A. S. & Roos, W. D. (2017). Chemical oxygen demands removal from electroplating wastewater by purified and polymer functionalized carbon nanotubes adsorbents. *Water Resour. Ind.*, 18, 33–50.
- Baqer, A. A., Matori, K. A., Al-Hada, N. M., Shaari, A. H., Saion, E. & Chyi, J. L.Y. (2017). Effect of polyvinylpyrrolidone on cerium oxide nanoparticles characteristics prepared by a facile heat treatment technique. *Results Physics*vol., 7 pp. 611-619.
- Baral, S. S., Mohanasundaram, K. & Ganesan, S. (2021) Selection of suitable adsorbent for the removal of Cr(VI) by using objective based multiple attribute decision making method. *Preparative Biochemistry & Biotechnology*, 51,1, pp. 69-75, doi: [10.1080/10826068.2020.1789993](https://doi.org/10.1080/10826068.2020.1789993).
- Dave, P. N., Pauline, L. S. & David, G. K. *Source and behaviour of arsenic in natural waters*. British Geological Survey, Wallingford, Oxon OX10 8BB, U.K. 261(2002)
- Dey, S. & Islam, A. (2015). A review on textile wastewater characterization in Bangladesh. *Res. Environ.*, 5, pp. 15–44.
- Deziel, N. C. & Villanueva, C. M. (2024). Assessing exposure and health consequences of chemicals in drinking water in the 21st Century. *J Expo Sci Environ Epidemiol*, 34, pp. 1–2, <https://doi.org/10.1038/s41370-024-00639-0>.
- Eddy, N. O., Garg, R., Garg, R., Aikoye, A. & Ita, B. I. (2023a). Waste to resource



- recovery: mesoporous adsorbent from orange peel for the removal of trypan blue dye from aqueous solution. *Biomass Conversion and Biorefinery*, 13, pp. 13493-13511, doi: 10.1007/s13399-022-02571-5.
- Eddy, N. O., Ukpe, R. A., Ameh, P., Ogbodo, R., Garg, R. & Garg, R. (2023). Theoretical and experimental studies on photocatalytic removal of methylene blue (MetB) from aqueous solution using oyster shell synthesized CaO nanoparticles (CaONP-O). *Environmental Science and Pollution Research*, <https://doi.org/10.1007/s11356-022-22747-w>.
- Eddy, N. O. & Garg, R. (2021). CaO nanoparticles: Synthesis and application in water purification. Chapter 11. In: Handbook of research on green synthesis and applications of nanomaterials. Garg, R., Garg, R. and Eddy, N. O, edited. Published by IGI Global Publisher. DOI: 10.4018/978-1-7998-8936-6
- Eddy, N. O., Jibrin, J. I., Ukpe, R. A., Odiongenyi, A. O., Kasiemobi, A. M., Oladele, J. O. & Runde, M. (2024). Experimental and Theoretical Investigations of Photolytic and Photocatalysed Degradations of Crystal Violet Dye (CVD) in Water by oyster shells derived CaO nanoparticles (CaONP), *Journal of Hazardous Materials Advances*, 100413, <https://doi.org/10.1016/j.hazadv.2024.100413>.
- Garg, R., Garg, R., Eddy, N. O., Almohana, A. I., Fahad, S., Khan, M. A. & Hong, S. H. (2022). Biosynthesized silica-based zinc oxide nanocomposites for the sequestration of heavy metal ions from aqueous solutions. *Journal of King Saud University-Science* <https://doi.org/10.1016/j.jksus.2022.101996>
- Gougazeh, M. & Buhl, J. C. (2014). Synthesised and characterization of zeolite a by hydrothermal transformation of natural Jordanian kaolin, *J. Assoc. Arab Univ. Basic Appl. Sci.*, 15, pp. 35-42.
- Ibrahim, M. B. & Abdullahi, S.H. (2017). Green Synthesis of Zinc nanoparticles using *Ipomoea asarifolia* Leave extract and it's adsorbition properties for the removal of dyes. *Bayero Journal of Pure and Applied Science*, 10, 1, pp. 7-14.
- Jimor, W. O. & Umar, M. I. (2015). Determination of trace metal concentration in drinking water samples from Sani Mainagge Quarters, Gwale Local Government Area, Kano State, Nigeria. *International Journal of Science Research in Environmental Sciences*. 3, 9, pp. 0341-0349, 2015. <http://www.205pub.com/IJRes>.
- Lee, P. J., Saion, E., Al-Hada, N. M. & Soltani, N. (2015). A simple up-scalable Thermal treatment method for synthesis of zinc oxide nanoparticles. *Metals* 5, 4, pp.2383–2392.
- Makarov, V. V., Love, A. J., Sinitsyna, O.V., Makarova, S. S., Yaminsky, I. V. & Taliansky M. E (2014). "Green" Nanotechnologies: Synthesis of Metal Nanoparticles Using Plants. *Acta Naturae* 6: 35–44.
- Odoemelam, S. A., Oji, E. O., Eddy, N. O., Garg, R., Garg, R., Islam, S., Khan, M. A., Khan, N. A. & Zahmatkesh, S. (2023). Zinc oxide nanoparticles adsorb emerging pollutants (glyphosate pesticide) from aqueous solution. *Environmental Monitoring and Assessment*, <https://doi.org/10.1007/s10661-023-11255-0>.
- Sherifat, A., Abdulkarim, A. S., Abdulsalam, K. & Olalokan, D. (2019). Development of nano-silver doped zeolite A synthesized from Nigerian Ahkoro kaolin for treatment of waste water of a typical textile company. *A journal of Chemical Engineering communication*:207(8):1-24.



Tijani, J. O, Fatoba, O. O, Madzivire, G. & Petrik, L. F (2014). A Review of combined advanced oxidation technologies for the removal of organic pollutants from water. *Water Air Soil Pollut*, 225, doi 10.1007/s11270-014-2102.

Wang, T., Lin, J., Chen, Z., Megharaj, M., and Naidu, R. (2014). Green synthesized iron nanoparticles by green tea and eucalyptus leaves extracts used for removal of nitrate in aqueous solution. *J. Cleaner Prod.*, 83, pp. 413–419.

Ugya, A. Y., Imam, T. S. & Ajibade, F. O. (2017). Remediation of refinery wastewater using Electrocoagulation process. *Bayero Journal of Pure and Applied Sciences*, 10, 1, pp. 57-61.

Yusuf-Alaya, S. (2014). Synthesis, intercalation and characterization of zeolite A for adsorption studies of methylene blue, 22–45. (Master's thesis, Federal University

of Technology, Minna, Niger state, Nigeria).

### **Compliance with Ethical Standards Declarations**

The authors declare that they have no conflict of interest.

### **Data availability**

All data used in this study will be readily available to the public.

### **Consent for publication**

Not Applicable

### **Availability of data and materials**

The publisher has the right to make the data Public.

### **Competing interests**

The authors declared no conflict of interest.

### **Funding**

There is no source of external funding

